Numerical modelling concepts for tsunami warning systems

T. S. Murty, A. D. Rao, N. Nirupama and I. Nistor*

Since the four global oceans are not simply connected in the hydrodynamic sense, separate tsunami warning systems are needed for each ocean. Each ocean shows somewhat different tsunami characteristics, and for this reason, numerical models that are required for the tsunami warning system, also have to be different. These differences stem from whether an ocean gives rise to ocean-wide tsunamis or just to local tsunamis, and also the role played by boundary reflections. Using the concept of method of characteristics it is shown that the hyperbolic, parabolic, elliptic and parabolic–elliptic approaches are respectively valid for the Pacific, Atlantic, Indian and Arctic oceans.

Keywords: Closed system, open system, partially open system, numerical modelling, tsunami warning system.

AFTER the extremely disastrous tsunami of 26 December 2004 in the Indian Ocean, there has been a suggestion by the United Nations Organizations to establish a global tsunami warning system. This concept has no merit as can be seen from the fact that the four global oceans are not well connected (Figure 1). The Pacific, Atlantic and Indian oceans are connected in the south, through what is unofficially referred to as the Southern Ocean. The Pacific and Atlantic oceans are connected in the north to the Arctic Ocean. The Arctic and Indian oceans are not connected, at least directly. While it may be possible, at least in principle, to establish a global weather forecasting system, which is feasible because the atmosphere is continuous, this is not true for the tsunami warning system.

Besides the technical issue of four separate ocean basins, there is the more practical issue of different countries bordering different oceans. A realistic approach is four separate tsunami warning systems, one for each ocean basin.

After the damaging Aleutian earthquake tsunami of 1 April 1946, the Pacific tsunami warning system was established in 1949 in Hawaii. Until now there have been no tsunami warning systems for the Atlantic and Indian oceans, because tsunamis occur infrequently in these oceans. However, following the major tsunami in the Indian Ocean on 26 December 2004, tsunami warning systems are now being developed for the Indian and Atlantic oceans. At present, there is no priority for establishing a tsunami warning system for the Arctic Ocean, mainly because of low population density around its rim.

T. S. Murty and I. Nistor are in the Department of Civil Engineering, University of Ottawa, Ottawa, Canada; A. D. Rao is in the Centre for Atmospheric Sciences, Indian Institute of Technology, New Delhi 110 016, India; N. Nirupama is in the Disaster and Emergency Studies, Brandon University, Brandon, Canada.
*For correspondence. (e-mail: adrao@cas.iitd.ernet.in)

Tsunami characteristics of the four oceans

Table 1 summarizes the tsunami characteristics for the Pacific, Atlantic, Indian and Arctic oceans. Specifically, some 21 tsunami parameters are compared and contrasted.

Out of the four oceans, the Pacific is the largest and contains converging tectonic plate boundaries, which give rise to tsunamigenic earthquakes, and trans-oceanic as well as local tsunamis. As can be seen from Figure 2, tsunami travel times in the Pacific could be as high as 23 h. Hence, except for locally generated tsunamis, there is generally sufficient time to provide a warning, and if needed, evacuate the population to safe areas. Usually there are up to seven waves in a tsunami event, and sometimes even ten. Usually the wave with the highest amplitude is among the 3rd to 5th. Dissipation of tsunami energy due to frequency dispersion during propagation is noticeable. Due to its vastness, reflected waves from far-off coastlines, do not contribute in any significant manner to the water levels associated with the tsunami event[1].

In contrast, the Atlantic Ocean does not contain major converging tectonic plate boundaries. The mid-Atlantic

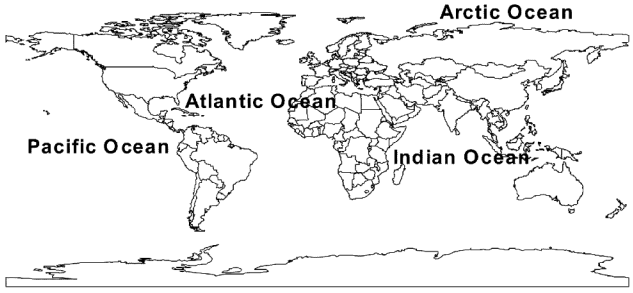

Figure 1. The four global oceans.

Table 1. Tsunami characteristics of the four oceans

Parameter	Pacific Ocean	Atlantic Ocean	Indian Ocean	Arctic Ocean
Area (km^2)	166,241,000	86,557,000	73,427,000	9,485,000
Average depth (m)	4188	3735	3872	1038
Deepest point (m)	Mariana Trench, 11,033	Puerto Rico Trench, 8648	Java Trench, 7725	Eurasian Basin, 5450
Number of trenches	18	3	1	None
Unpopulated area (%) – Southern Ocean	~20	30	55	Almost all of it
Length scale available (km). Half the side of an equivalent (in area) square	6447	4642	4284; if we omit the unpopulated area, it is about 2000	1540
Ocean-wide tsunamis	Yes	No	Yes	Rare – extremely strong dissipative influence by ice cover
Tectonic-converging plates producing tsunamigenic earthquakes	Yes	No; at mid-Atlantic ridge, the plates are diverging	Yes	Some, but not as strong as in the Pacific and Indian oceans
Frequency of tsunami occurrence	High	Rare	Rare	Rare
Frequency dispersion	High	N/A – since no ocean-wide tsunamis	Low	Small
Amplitude dispersion (nonlinear effects at the coast)	High	High	High	Moderate; ice cover does not permit significant amplification of tsunami waves at the coast
Tsunami travel times	Up to 23 h	Only local tsunamis which travel within minutes	Up to 10 h to most populated area	Local tsunamis; several minutes to atmost a couple of hours
Available warning time to most populated areas	Generally sufficient	Because of local tsunamis, only several minutes	1 to 4 h	Small – mostly several minutes
Importance of initial conditions	High	High	High	High
Importance of boundary reflections	Low	Low, since tsunamis originate close to the coast	High	Moderate; ice cover does not allow significant reflection of waves
Relevance of boundary conditions	Low	Medium	High	Medium
Effect of Coriolis force	Noticeable	Highly noticeable	Noticeable	High, since Coriolis force is strong
Type of boundary conditions to be used	Radiation type	Not important, since tsunamis are local	Reflective boundaries	Combination of radiative and reflective boundaries
Initial withdrawal of the ocean	Sometimes at some locations	Rare	Sometimes at some locations	Not obvious due to ice cover
Which wave is the highest	Among 3rd to 5th	Usually 1st wave	Usually 2nd wave	Usually 1st or 2nd wave
Nature of physical process	Hyperbolic (like astrology): everything is determined at birth	Parabolic: tsunamis travel slowly in shallow water near the coast. It is like a slow diffusion process	Elliptic: tsunami behaviour everywhere in the ocean, including reflections at the boundaries is relevant everywhere else	Half way between parabolic and elliptic

ridge is a diverging plate boundary, which generates new ocean floor, but no tsunamigenic earthquakes. Unlike the Pacific Ocean, which has on an average six tsunamis per year (most of them small), in the Atlantic Ocean tsunami events are rare. Two local tsunamis occurred in the 20th century. One on the western side of north Atlantic, off the coast of Newfoundland, Canada, November 1929 and the other on the eastern side of north Atlantic, near Portugal in

February 1969. Not only are Atlantic tsunamis rare, they also do not propagate over long distances and dissipate rather quickly in time and space. Thus unlike the Pacific Ocean, there are no tsunamis racing across the Atlantic Ocean[2,3].

The Indian Ocean is similar to the Pacific in several respects, but also with some important differences. Like the Pacific, the Indian Ocean also contains converging tectonic plate boundaries, tsunamigenic earthquakes and ocean-wide as well as local tsunamis. Figure 3 illustrates a tsunami travel time chart for Mumbai, India.

However, important differences with the Pacific Ocean include: Rarity of tsunami occurrences, important role played by boundary reflections, and small dissipation of tsunami energy due to frequency dispersion during propagation[4–9].

Finally, the ice-bound Arctic Ocean is quite different from the other three oceans. Here also, tsunamis are infrequent and mostly local. The ice cover exerts a great influence on the tsunami, which is a long gravity wave. The coastal inundation aspects in the Arctic Ocean are different from those of the other three oceans, because of shore fast ice. Also being situated entirely in high latitudes of the northern hemisphere, the Coriolis effects on tsunami propagation are strong.

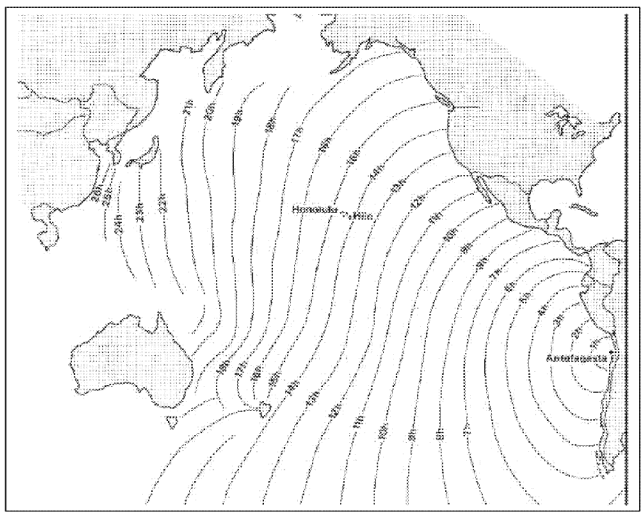

Figure 2. Tsunami travel time chart for the Pacific Ocean.

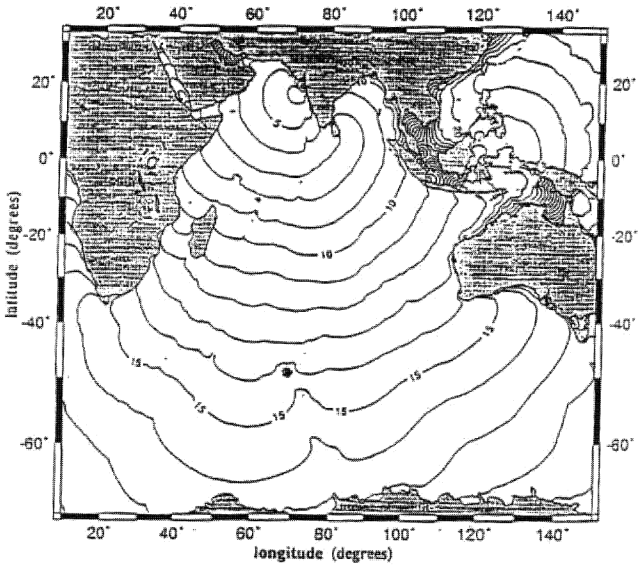

Figure 3. Travel time chart for Mumbai, India. The contours are of 1 h interval.

Numerical modelling concepts

Making use of the concept of the method of characteristics[6,9,10–12] physical processes can be broadly classified into the following three categories: hyperbolic (open system), parabolic (partially open system), and elliptic (closed system). In the hyperbolic problem, which is also referred to as the marching problem, the solution marches out with initially imposed conditions. Radiative boundary conditions are usually used for these problems.

In the elliptic method, which is also called the jury problem, not only the initial conditions, but also the boundary conditions play an important role. The parabolic method is somewhat between the hyperbolic and elliptic methods. Based upon the physical characteristics of the tsunamis (Table 1) and the mathematical concepts mentioned above, it becomes obvious that the following methods respectively could be used for the four global oceans for numerical modelling of the tsunami warning systems: Pacific (hyperbolic), Atlantic (parabolic), Indian (elliptic) and Arctic (parabolic–elliptic).

Based on the above considerations, it is suggested that the following is an appropriate approach for numerical modelling of tsunami warning systems. For the Pacific Ocean which generates trans-oceanic tsunamis, boundary reflections do not play a significant role, the hyperbolic method is relevant, in which the initial conditions are of paramount importance. Figure 4 *a* schematically illustrates this.

In the Atlantic Ocean, there are no major convergent tectonic plate boundaries to give rise to tsunamigenic earthquakes[2]. Rather, the mid-Atlantic ridge is a divergent plate boundary. Hence tsunamis are rare here, and the few that occur are almost always local and originate near the coastlines. Since tsunamis travel slowly in shallow water, tsunami propagation in the Atlantic Ocean is more like a slow diffusion and hence the appropriate method is parabolic. This is schematically illustrated in Figure 4 *b*.

In the Indian Ocean, boundary reflections contribute significantly to the water levels associated with the tsunami waves[4,5]. For this reason the elliptic approach is most appropriate. This is schematically illustrated in Figure 4 *c*.

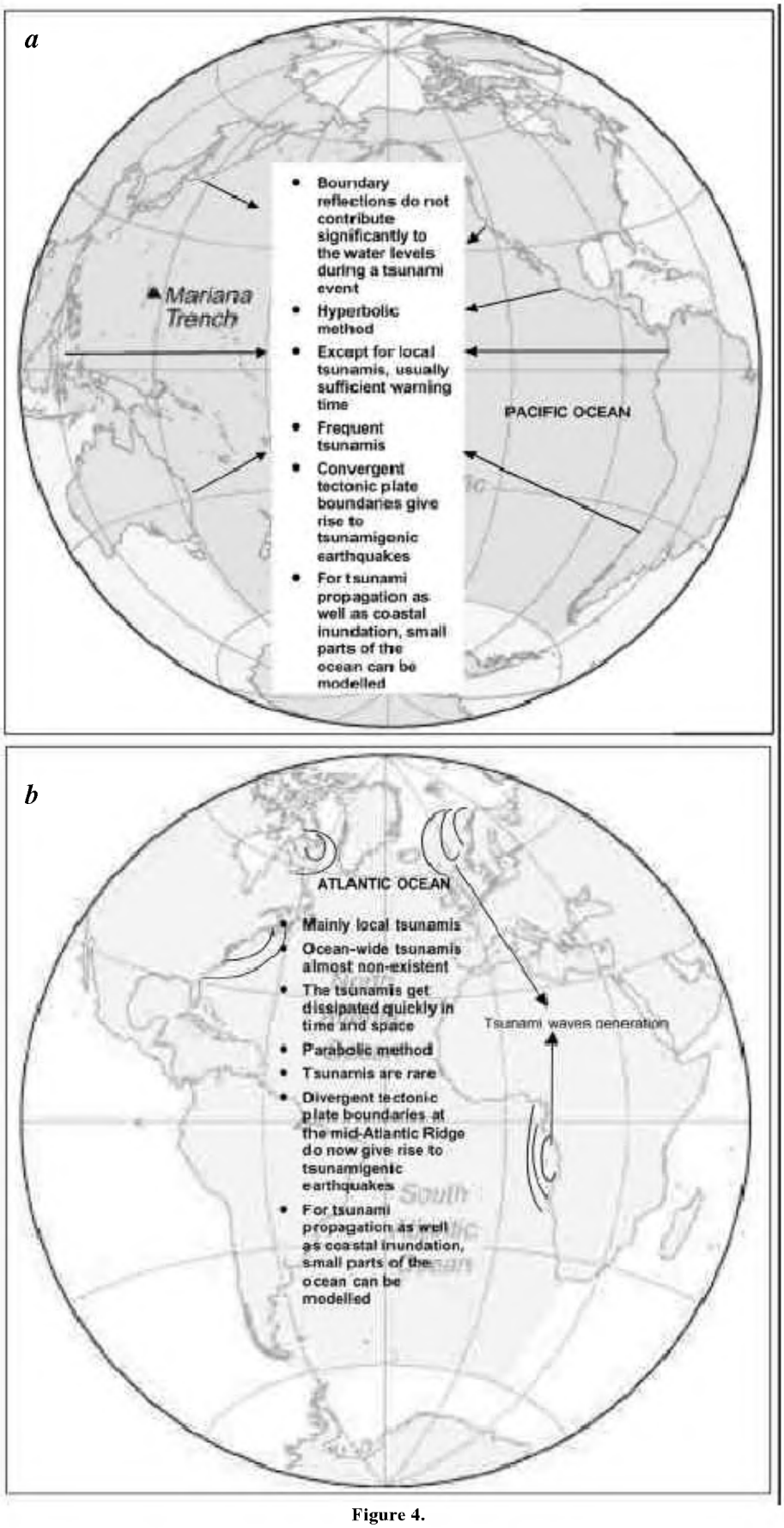

Figure 4.

(*Contd...*)

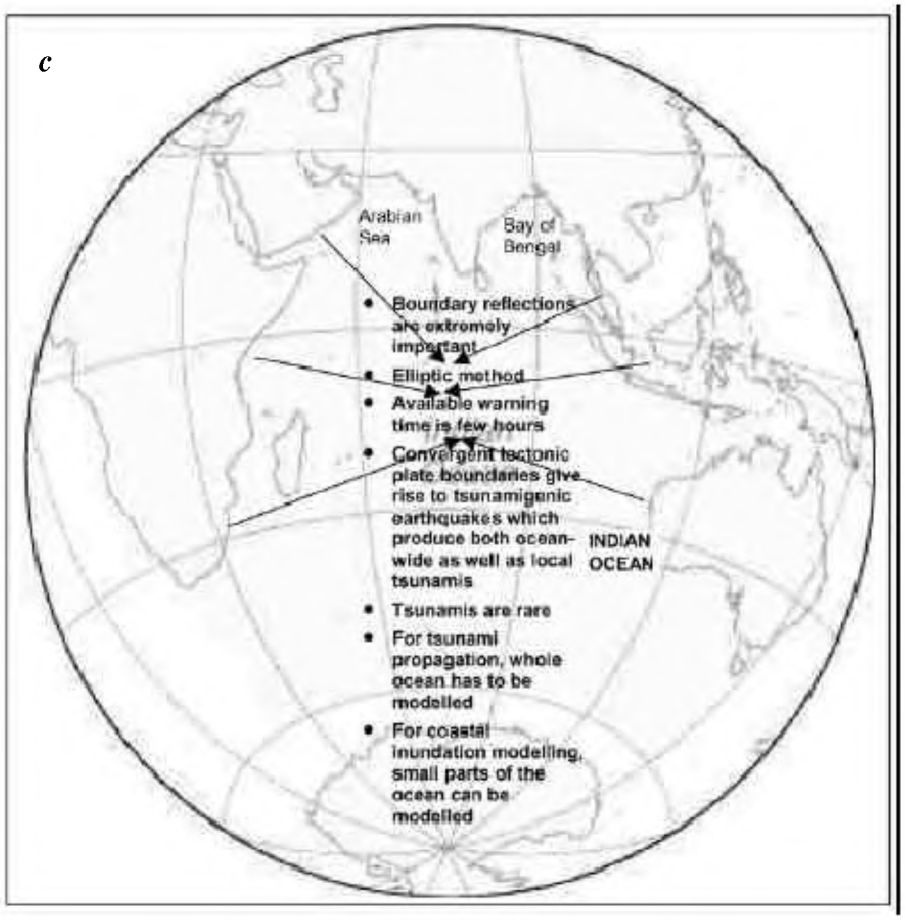

Figure 4. Schematic illustration of the tsunami numerical modelling concept for (*a*) Pacific Ocean, (*b*) Atlantic Ocean and (*c*) Indian Ocean.

There are indications that in the recent Indian Ocean tsunami of 26 December 2004, the ocean thermal structure did indeed play an important role. Internal waves owe their existence to density variations, and an analysis of the observed data on the maximum amplitudes of the tsunami does suggest that some of the very large tsunami amplitudes (up to 8 m) probably could not have been possible without the amplification due to coupling between the surface tsunami and the internal waves below. This effect is most noticeable for parts of the Tamil Nadu coast, Sri Lanka and the Andaman and Nicobar Islands.

The types of boundary conditions to be used are different for each ocean. For the Pacific Ocean, radiation-type boundary condition is most appropriate, since reflected waves are not important, and hence the solution can march out of the domain. On the other hand, for the Indian Ocean, waves reflected from the boundaries do interact with the direct tsunami waves in determining the total water levels. For this reason, reflective boundaries need to be specified. For the Atlantic Ocean, absorption-type boundary condition is most relevant as tsunami waves actually originate near the boundaries and propagate into the deep ocean.

Since reflected waves play an important role in tsunamis in the Indian Ocean, data requirements for modelling tsunamis in the Indian Ocean are much more stringent than the other oceans. First, the deep ocean bathymetry itself needs to be more detailed than the currently available ETOPO2 bathymetry, which provides data at 2 min of arc resolution. We need data at least at the resolution of 1 min of arc, and if possible even at a better resolution. Since coastal reflections must be included in coastal inundation modelling, topographic and land orographic data must be available at a resolution of 10 m, if possible. Hence, in summary, the tsunami models for the Indian Ocean require much more detailed coastal topographic data as well as ocean bathymetric data.

Tsunami propagation

Since tsunamis propagate over trans-oceanic distances, the curvature of the earth must be taken into account in numerical models for tsunami propagation. Hence the governing equations should be written in a spherical polar coordinate system, rather than in the traditional Cartesian coordinates. Following Kowalik and Murty[13], the basic equations can be written as follows.

Whenever fluid motions are considered along large distances on the globe, the equation of motion and continuity

can be written in spherical polar coordinates λ, ϕ and R, defined as longitude, latitude and distance from the earth's centre. If the origin of the system is located on the ocean surface, it is more suitable to introduce a vertical coordinate $z = R - R_0$. Here R_0 is the radius of the earth and is equal to 6370 km.

Because the earth does not exactly have a spherical shape, the equation given below will better describe the large-scale motion relative to the geopotential and not the spherical surfaces.

The equations of motion in the spherical system are:

$$\frac{Du}{Dt} - \left(2\Omega + \frac{u}{R\cos\phi}\right)(v\sin\phi - w\cos\phi) = -\frac{1}{\rho R\cos\phi}\frac{\partial p}{\partial\lambda} + A_\lambda, \tag{1}$$

$$\frac{Dv}{Dt} + \frac{wv}{R} + \left(2\Omega + \frac{u}{R\cos\phi}\right)u\sin\phi = -\frac{1}{\rho R}\frac{\partial p}{\partial\phi} + A_\phi, \tag{2}$$

$$\frac{Dw}{Dt} - \frac{v^2}{R} - \left(2\Omega + \frac{u}{R\cos\phi}\right)u\cos\phi = -\frac{1}{\rho}\frac{\partial p}{\partial z} - g + A_z, \tag{3}$$

where A_λ, A_ϕ, and A_z are the components of the viscous force, and the time operator expressed as

$$\frac{D}{Dt} = \frac{\partial}{\partial t} + \frac{u}{R\cos\phi}\frac{\partial}{\partial\lambda} + \frac{v}{R}\frac{\partial}{\partial\phi} + w\frac{\partial}{\partial z}. \tag{4}$$

The frictional forces are written in a somewhat complicated form:

$$A_\lambda = A_1 u - \frac{N_h}{R^2\cos^2\phi}\left(u + 2\frac{\partial}{\partial\lambda}(v\sin\phi - w\cos\phi)\right), \tag{5}$$

$$A_\phi = A_1 v + N_h\left(-\frac{v}{R^2\cos^2\phi} + \frac{2\sin\phi}{R^2\cos^2\phi}\frac{\partial u}{\partial\lambda} + \frac{2}{R^2}\frac{\partial w}{\partial\phi}\right), \tag{6}$$

$$A_z = A_1 w + N_h\left(-\frac{2w}{R^2} - \frac{2}{R^2\cos^2\phi}\frac{\partial u}{\partial\lambda} - \frac{2}{R^2\cos^2\phi}\frac{\partial}{\partial\lambda}(v\cos\phi)\right), \tag{7}$$

where the operator A_1 has the following form,

$$A_1 = N_h\left(\frac{1}{R^2\cos^2\phi}\frac{\partial^2}{\partial\lambda^2} + \frac{1}{R^2\cos^2\phi}\frac{\partial}{\partial\phi}\left(\cos\phi\frac{\partial}{\partial\phi}\right)\right) + \frac{\partial}{\partial z}\left(N_z\frac{\partial}{\partial z}\right). \tag{8}$$

The equation of continuity in the spherical system is

$$\frac{1}{R\cos\phi}\frac{\partial u}{\partial\lambda} + \frac{1}{R\cos\phi}\frac{\partial}{\partial\phi}(v\cos\phi) + \frac{\partial w}{\partial z} = 0. \tag{9}$$

Finally, the equation for diffusion can be expressed in the following way:

$$\frac{Dc}{Dt} = A_2 c, \tag{10}$$

where operator A_2 is

$$A_2 = D_h\left(\frac{1}{R^2\cos^2\phi}\frac{\partial^2}{\partial\lambda^2} + \frac{1}{R^2\cos\phi}\frac{\partial}{\partial\phi}\left(\cos\phi\frac{\partial}{\partial\phi}\right)\right) + \frac{\partial}{\partial z}\left(D_z\frac{\partial}{\partial z}\right). \tag{11}$$

Variable c stands for concentration, and it can denote salinity, temperature or any passive admixture in sea water.

The temperature and density fields become relevant if internal waves play a role in the coastal effects of the tsunami. It has been suggested that some of the coastal amplification of the 26 December 2004 tsunami in the Indian Ocean, could have been due to the interaction between the tsunami waves and the internal waves.

Coastal inundation

Since regular grids in a finite difference framework cannot properly resolve the extreme complexity of the coastline geometry, a more appropriate approach is to use a finite element model with irregular triangular grids. Here we will briefly describe the so-called ADCIRC model, which is a finite element model for the computation of storm surges. With some modifications, this model can be adapted for the computation of coastal inundation from tsunamis.

In a series of reports and papers[12,14–21], the so-called ADCIRC model of the US Army Corps of Engineers has been described. The following material is based on Westerink *et al.*[21]. ADCIRC stands for 'An advanced three-dimensional circulation model for shelves, coasts and estuaries'. The ADCIRC-2DDI is a depth-integrated option of a system of two and three-dimensional hydrodynamic codes of ADCIRC.

ADCIRC-2DDI uses the depth-integrated equations of mass and momentum conservation, subject to the incom-

pressibility, Boussinesq, and hydrostatic pressure approximations. Using the standard quadratic parameterization for bottom stress and neglecting baroclinic terms and lateral diffusion/dispersion effects leads to the following set of conservation statements in primitive non-conservative form, expressed in a spherical coordinate system[7,22]:

$$\frac{\partial \zeta}{\partial t}+\frac{1}{R\cos\varphi}\left[\frac{\partial UH}{\partial \lambda}+\frac{\partial (VH\cos\varphi)}{\partial \varphi}\right]=0, \tag{12}$$

$$\begin{aligned}&\frac{\partial U}{\partial t}+\frac{1}{R\cos\varphi}U\frac{\partial U}{\partial \lambda}+\frac{1}{R}V\frac{\partial U}{\partial \varphi}-\left(\frac{\tan\varphi}{R}U+f\right)V\\&\quad=-\frac{1}{R\cos\varphi}\frac{\partial}{\partial \lambda}\left[\frac{p_s}{\rho_0}+g(\zeta-\eta)\right]+\frac{\tau_{s\lambda}}{\rho_0 H}+-\tau_* U,\end{aligned} \tag{13}$$

$$\begin{aligned}&\frac{\partial V}{\partial t}+\frac{1}{R\cos\varphi}U\frac{\partial V}{\partial \lambda}+\frac{1}{R}V\frac{\partial V}{\partial \varphi}+\left(\frac{\tan\varphi}{R}U+f\right)U\\&\quad=-\frac{1}{R}\frac{\partial}{\partial \varphi}\left[\frac{p_s}{\rho_0}+g(\zeta-\eta)\right]+\frac{\tau_{s\varphi}}{\rho_0 H}+-\tau_* V,\end{aligned} \tag{14}$$

where t is the time, λ, ϕ the degrees longitude (east of Greenwich positive) and degrees latitude (north of the equator positive), ζ the free surface elevation relative to the geoid, U, V the depth-averaged horizontal velocities, R the radius of the earth, $H = \zeta + h$, the total water column, h the bathymetric depth relative to the geoid, $f = 2\,\Omega \sin\phi$, the Coriolis parameter, Ω the angular speed of the earth, P_s is atmospheric pressure at the free surface, g the acceleration due to gravity, η the effective Newtonian equilibrium tide potential, ρ_0 the reference density of water and $\tau_{s\lambda}$, $\tau_{s\phi}$ the applied free surface stresses

$$\tau_* = C_f\frac{(U^2+V^2)^{1/2}}{H},$$

where C_f is the bottom friction coefficient.

A practical expression for the effective Newtonian equilibrium tide potential as given by Reid[23] is:

$$\eta(\lambda,\varphi,t)=\sum_{n.j}\alpha_{jn}C_{jn}f_{jn}(t_0)L_j(\varphi)\cos\left[\frac{2\pi(t-t_0)}{T_{jn}+j\lambda+V_{jn}(t_0)}\right], \tag{15}$$

where C_{jn} is the constant characterizing the amplitude of tidal constituent n of species j, α_{jn} the effective earth elasticity factor for tidal constituent n of species j, f_{jn} the time-dependent nodal factor, V_{jn} the time-dependent astronomical argument, $j = 0, 1, 2$, the tidal species ($j = 0$, declinational; $j = 1$, diurnal; $j = 2$, semidiurnal), $L_0 = 3\sin^2\phi - 1$, $L_1 = \sin(2\phi)$, $L_2 = \cos^2(\phi)$, λ, ϕ the degrees longitude and latitude respectively, t_0 the reference time and T_{jn} the period of constituent n of species j.

Values for C_{jn} are presented by Reid[23]. The value for the effective earth elasticity factor is typically taken as 0.69 for all tidal constituents[9,24], although its value has been shown to be slightly constituent-dependent. To facilitate a finite element solution to eqs (12) to (14), these equations are mapped from spherical form into a rectilinear coordinate system using a Carte Parallelogrammitque (CP) projection[25]:

$$x' = R(\lambda-\lambda_0)\cos\varphi_0, \tag{16}$$

$$y' = R\varphi, \tag{17}$$

where λ_0, ϕ_0 is the centrepoint of the projection. Applying the CP projection to eqs (12) to (14) gives the shallow-water equations in primitive non-conservative form expressed in the CP coordinate system:

$$\frac{\partial \zeta}{\partial t}+\frac{\cos\varphi_0}{\cos\varphi}\frac{\partial (UH)}{\partial x'}+\frac{1}{\cos\varphi}\frac{\partial (VH\cos\varphi)}{\partial y'}=0, \tag{18}$$

$$\begin{aligned}&\frac{\partial U}{\partial t}+\frac{\cos\varphi_0}{\cos\varphi}U\frac{\partial U}{\partial x'}+V\frac{\partial U}{\partial y'}-\left(\frac{\tan\varphi}{R}U+f\right)V\\&\quad=-\frac{\cos\varphi_0}{\cos\varphi}\frac{\partial}{\partial x'}\left[\frac{p_s}{\rho_0}+g(\zeta-\eta)\right]+\frac{\tau_{s\lambda}}{\rho_0 H}-\tau_* U,\end{aligned} \tag{19}$$

$$\begin{aligned}&\frac{\partial V}{\partial t}+\frac{\cos\varphi_0}{\cos\varphi}U\frac{\partial V}{\partial x'}+V\frac{\partial U}{\partial y'}-\left(\frac{\tan\varphi}{R}U+f\right)U\\&\quad=-\frac{\partial}{\partial y'}\left[\frac{p_s}{\rho_0}+g(\zeta-\eta)\right]+\frac{\tau_{s\varphi}}{\rho_0 H}-\tau_* V.\end{aligned} \tag{20}$$

Utilizing the finite element method to resolve the spatial dependence in the shallow-water equations in their primitive form gives inaccurate solutions with severe artificial $2.\Delta x$ modes. However, reformulating the primitive equations into a GWCE (Generalized Wave Continuity Equation) form gives highly accurate, noise-free, finite element-based solutions to the shallow-water equations[26,27]. The GWCE is derived by combining a time-differentiated form of the primitive continuity equation and a spatially differentiated form of the primitive momentum equations recast into conservative form, reformulating the convective terms into non-conservative form and adding the primitive form of the continuity equation multiplied by a constant in time and space[16,26], τ_0. The GWCE in the CP coordinate system is:

$$\frac{\partial^2}{\partial t^2}+\tau_0\frac{\partial \zeta}{\partial t}+\frac{\cos\varphi_0}{\cos\varphi}\frac{\partial}{\partial x'}\frac{\partial \zeta}{\partial t}$$

$$\left\{\begin{array}{l} U-\dfrac{\cos\varphi_0}{\cos\varphi}UH\dfrac{\partial U}{\partial x'}-VH\dfrac{\partial U}{\partial y'}+\left(\dfrac{\tan\varphi}{R}U+f\right)VH \\ -H\dfrac{\cos\varphi_0}{\cos\varphi}\dfrac{\partial}{\partial x'}\left[\dfrac{p_s}{\rho_0}+g(\varsigma-\eta)\right]-(\tau_*-\tau_0)UH+\dfrac{\tau_{s\lambda}}{\rho_0} \end{array}\right\}$$

$$+\frac{\partial}{\partial y'}\left\{\begin{array}{l} V\dfrac{\partial\varsigma}{\partial t}-\dfrac{\cos\varphi_0}{\cos\varphi}UH\dfrac{\partial V}{\partial x'}-VH\dfrac{\partial V}{\partial y'} \\ -\left(\dfrac{\tan\varphi}{R}U+f\right)UH \\ -H\dfrac{\partial}{\partial y'}\left[\dfrac{p_s}{\rho_0}+g(\varsigma-\eta)\right]-(\tau_*-\tau_0)VH+\dfrac{\tau_{s\varphi}}{\rho_0} \end{array}\right\}$$

$$-\frac{\partial}{\partial t}\left(\frac{\tan\varphi}{R}VH\right)+-\tau_0\left(\frac{\tan\varphi}{R}VH\right)=0. \qquad (21)$$

The GWCE (eq. 21) is solved in conjunction with the primitive momentum equations in non-conservative form (eqs (19) and (20)).

The high accuracy of GWCE-based finite element solutions is a result of their excellent numerical amplitude and phase propagation characteristics. In fact, Fourier analysis indicates that in constant-depth water and using linear interpolation, a linear tidal wave resolved with 25 nodes per wavelength is more than adequately resolved over the range of Courant numbers ($C = \sqrt{gh}\Delta t/\Delta x \leq 1.0$)[16]. Furthermore, the monotonic dispersion behaviour of GWCE-based finite element solutions avoids generating artificial near $2.\Delta x$ modes, which plague primitive-based finite element solutions[3,28]. The monotonic dispersion behaviour of GWCE-based finite element solutions are similar to that associated with staggered finite difference solutions to the primitive shallow-water equations that allow for extremely flexible spatial discretizations, which result in a highly effective minimization of the discrete size of any problem[8].

Details of ADCIRC and implementation of GWCE-based solution to the shallow-water equations are described by Luettich *et al.*[16]. As with most GWCE-based finite element codes, ADCIRC applies three-noded linear triangles for surface elevation, velocity and depth. Furthermore, the decoupling of the time and space discrete form of the GWCE and momentum equations, time-independent and/or tri-diagonal system matrices, elimination of spatial integration procedures during time-stepping, and full vectorization of all major loops result in a highly efficient code.

Summary

The four global oceans, namely the Pacific, Atlantic, Indian and Arctic, have different tsunami characteristics. Using the concept of the method of characteristics, it is suggested that the following methods be used respectively, for numerical models for tsunami warning systems: the hyperbolic method for the Pacific Ocean, parabolic for the Atlantic Ocean, elliptic for the Indian Ocean and the parabolic–elliptic for the Arctic Ocean.

1. Murty, T. S., *Seismic Seawaves – Tsunamis*, Bull. No. 198, Fisheries Research Board of Canada, Ottawa, 1977, p. 337.
2. Murty, T. S., Nirupama, N., Nistor, I. and Hamdi, S., Tsunamis in the Atlantic Ocean. *J. Indian Soc. Earthquake Technology* (submitted), 2005.
3. Foreman, M. G. G., An analysis of the 'Wave Equation' model for finite element tidal computations. *J. Comput. Phys.*, 1983, **52**, 290–312.
4. Murty, T. S., Nirupama, N., Nistor, I. and Hamdi, S., Far field characteristics of the tsunami of 26 December 2004. *J. Indian Soc. Earthquake Technol.* (accepted).
5. Murty, T. S., Rao, A. D. and Nirupama, N., Inconsistencies in travel times and amplitudes of the 26th December 2004 tsunami. *J. Mar. Med. Soc.*, 2005, **7**, 7–14.
6. Murty, T. S., Rao, A. D., Nirupama, N. and Nistor, I., Tsunami warning systems for the hyperbolic (Pacific), parabolic (Atlantic) and elliptic (Indian) oceans. *J. Indian Geophys. Union*, 2006, **10**, 69–78.
7. Flather, R. A., A numerical model investigation of tides and diurnal-period continental shelf waves along Vancouver Island. *J. Phys. Oceanogr.*, 1988, **18**, 115–139.
8. Foreman, M. G. G., A comparison of tidal models for the southwest coast of Vancouver Island. In Proc. 7th Int. Conf. on Comput. Methods in Water Resour, Elsevier, 1988.
9. Hendershott, M. C., Long waves and ocean tides. In *Evolution of Physical Oceanography* (eds Warren, B. A. and Wunsch, C.), MIT Press, Cambridge, Mass., 1981, pp. 292–346.
10. Murty, T. S., Storm surges – meteorological ocean tides. *Can. J. Fish. Aquat. Sci.*, 1984, **212**, 897.
11. Crandall, S. H., *Engineering Analysis – A Survey of Numerical Procedures*, McGraw Hill, New York, 1956, p. 417.
12. Ann, B. C., Modeling methodologies for the prediction of hurricane storm surge. In *Recent Advances in Marine Science and Technology* (ed. Saxena, N. K.), PACON International, Honolulu, 1997, pp. 177–189.
13. Kowalik, Z. and Murty, T. S., Numerical simulation of two-dimensional tsunami runup. *Mar. Geod.*, 1993, **16**, 87–100.
14. Cialone, M. A., Coastal Modelling System (CMS) User's Manual, Instruction Report CERC-91-1, Coastal Engineering Research Centre, US Army Engineer Waterways Experiment Station, Vicksburg, MS, USA, 1991.
15. Luettich, R. A., Westerink, J. J. and Scheffner, N. W., ADCIRC: An advanced three-dimensional circulation model for shelves, coasts and estuaries; Report 1: Theory and methodology of ADCIRD-2DDI and ADCIRC-3DL. Coastal Engineering Research Centre, US Army Engineer Waterways Experiment Station, Vicksburg, MS, USA, 1991.
16. Luettich, R. A., Westerink, J. J. and Scheffner, N. W., ADCIRC: An advanced three-dimensional circulation model for shelves, coasts and estuaries; Report 1: Theory and methodology of ADCIRD-2DDI and ADCIRC-3DL. Technical Report DRP Coastal Engineering Research Centre, US Army Engineer Waterways Experiment Station, Vicksburg, MS, USA, 1992.
17. Mark, D. J. and Scheffner, N. W., Validation of a continental-scale storm surge model for the coast of Delaware. Third International Conference on Estuarine and Coastal Modelling, Chicago, IL, 8–10 September 1993.
18. Scheffner, N. W., Mark, D. J., Blain, C. A., Westerink, J. J. and Luettich, R. A., ADCIRC – An advanced three-dimensional circu-

lation model for shelves, coasts and estuaries. Report 5. A tropical storm data base for the East and Gulf of Mexico coasts of the United States, Dredging Research Program, Technical Report DRP-92-6, US Army Corps of Engineers, Washington DC, USA, August 1994, 48 pages plus appendices.

19. Westerink, J. J., Luettich, R. A., Baptista, A. M., Scheffner, N. W. and Farrar, P., Tide and storm surge predictions using a finite element model. *J. Hydraul. Eng.*, 1992, **118**, 1373–1390.
20. Westerink, J. J., Luettich, R. A., Blain, C. A. and Scheffner, N. W., ADCIRC: An advanced three-dimensional circulation model for shelves, coasts and estuaries. Report 2: Users manual for ADCIRD-2DDI. Technical Report DRP-92-6, Coastal Engineering Research Centre, US Army Engineer Waterways Experiment Station, Vicksburg, MS, USA, 1993.
21. Westerink, J. J., Luettich, R. A. and Scheffner, N. W., ADCIRC: An advanced three-dimensional circulation model for shelves, coasts and estuaries. Report 3: Development of a tidal constituent database for the western North Atlantic and Gulf of Mexico. Technical Report DRP-92-6, Coastal Engineering Research Centre, US Army Engineer Waterways Experiment Station, Vicksburg, MS, USA, 1993.
22. Kolar, R. L., Gray, W. J., Westerink, J. J. and Luettich, R. A., Shallow water modelling in spherical coordinates: Equation formulation, numerical implementation, and application. *J. Hydraul. Res.*, 1994, **32**, 3–24.
23. Reid, R. O., *Water Level Changes, Handbook of Coastal and Ocean Engineering* (ed. Herbich, J.), Gulf Publishing, Houston, USA, 1990.
24. Schwiderski, E. W., On chanting global ocean tides. *Rev. Geophys. Space Phys.*, 1980, **18**, 243–268.
25. Pearson, F., *Map Projections: Theory and Applications*, CRC Press, Boca Raton, FL, USA, 1990.
26. Lynch, D. R. and Gray, W. G., A wave equation model for finite element tidal computation. *Comput. Fluids*, 1979, **7**, 207–228.
27. Kinnmark, I. P. E., The shallow water wave equations: formulations, analysis and application. Ph D dissertation, Princeton University, Princeton, NJ, USA, 1984.
28. Platzman, G. W., Some response characteristics of finite element tidal models. *J. Comput. Phys.*, 1981, **40**, 36–63.

Received 11 July 2005; revised accepted 12 January 2006